MycoKeys 90: 31–51 (2022)
doi: 10.3897/mycokeys.90.84717
https://mycokeys.pensoft.net

RESEARCH ARTICLE

A peer-reviewed open-access journal
MycoKeys
Launched to accelerate biodiversity research

Taxonomy and molecular phylogeny of *Trametopsis* (Polyporales, Basidiomycota) with descriptions of two new species

Shun Liu[1], Yi-Fei Sun[1], Yan Wang[1], Tai-Min Xu[1], Chang-Ge Song[1], Yuan-Yuan Chen[2], Bao-Kai Cui[1]

1 *Institute of Microbiology, School of Ecology and Nature Conservation, Beijing Forestry University, Beijing 100083, China* **2** *College of Forestry, Henan Agricultural University, Zhengzhou, Henan 450002, China*

Corresponding author: Bao-Kai Cui (cuibaokai@bjfu.edu.cn)

Academic editor: María P. Martín | Received 1 April 2022 | Accepted 17 May 2022 | Published 31 May 2022

Citation: Liu S, Sun Y-F, Wang Y, Xu T-M, Song C-G, Chen Y-Y, Cui B-K (2022) Taxonomy and molecular phylogeny of *Trametopsis* (Polyporales, Basidiomycota) with descriptions of two new species. MycoKeys 90: 31–51. https://doi.org/10.3897/mycokeys.90.84717

Abstract

Trametopsis is a worldwide genus belonging to Irpicaceae in the phlebioid clade, which can cause a white decay of wood. Previously, only three species were ascribed to the genus. In this study, we performed a morphological and phylogenetic study of *Trametopsis*. Molecular phylogenetic analyses of multiple loci included the internal transcribed spacer (ITS) regions, the large subunit nuclear ribosomal RNA gene (nLSU), the largest subunit of RNA polymerase II (RPB1), the second largest subunit of RNA polymerase II (RPB2) and the translation elongation factor 1-α gene (TEF1). Phylogenetic trees were inferred from the combined datasets of ITS+nLSU sequences and ITS+nLSU+RPB1+RPB2+TEF1 sequences by using maximum parsimony, maximum likelihood and Bayesian inference analyses. Combined with molecular data, morphological characters and ecological traits, two new species of *Trametopsis* are discovered. *Trametopsis abieticola* is characterised by its pileate, solitary or imbricate basidiomata, buff to buff-yellow pileal surface when fresh, becoming pinkish buff to clay-buff when dry, cream to buff pore surface when fresh, becoming pinkish buff to greyish brown upon drying, round to angular and large pores (0.5–1 per mm), cylindrical basidiospores (5.8–7.2 × 1.9–2.6 μm), distributed in the high altitude of mountains and grows on *Abies* sp. *Trametopsis tasmanica* is characterised by its resupinate basidiomata, cream to pinkish-buff pore surface when fresh, becoming honey-yellow to snuff brown upon drying, cylindrical basidiospores (5.2–6.3 × 1.8–2.2 μm), and by growing on *Eucalyptus* sp. Detailed descriptions and illustrations of the two novel species are provided.

Keywords

Irpicaceae, macrofungi, multi-gene phylogeny, new species, white-rot fungi

Copyright *Shun Liu et al.* This is an open access article distributed under the terms of the Creative Commons Attribution License (CC BY 4.0), which permits unrestricted use, distribution, and reproduction in any medium, provided the original author and source are credited.

Introduction

Trametopsis Tomšovský was established by Tomšovský (2008) with *T. cervina* (Schwein.) Tomšovský as type species. The morphological characteristics of *Trametopsis* are as follows: Basidiomata annual, sessile to effused-reflexed or rarely resupinate. Pileal surface pinkish buff to cinnamon or clay-buff, hirsute to strigose. Pore surface concolorous with pileal surface; pores irregular, daedaloid to irpicoid; dissepiments thin and lacerate. Context pale buff, fibrous. Tubes concolorous with the context, corky. Hyphal system dimitic; generative hyphae clamped. Cystidia absent; fusoid cystidioles occasionally present. Basidia clavate, bearing four sterigmata and a basal clamp connection. Basidiospores cylindrical, hyaline, thin-walled, smooth, IKI–, CB– (Tomšovský 2008).

Gómez-Montoya et al. (2017) evaluated the species of *Trametopsis* in the Neotropics based on phylogenetic evidences and morphological analyses. The phylogenetic analyses showed that *Trametopsis* is an independent genus; furthermore, one new species, *T. aborigena* Gómez-Mont. & Robledo, and the two new combinations, *T. brasiliensis* (Ryvarden & de Meijer) Gómez-Mont. & Robledo and *T. luteocontexta* (Ryvarden & de Meijer) Gómez-Mont., Robledo & Drechsler-Santos were presented. Westphalen et al. (2019) summarised *Antrodiella* Ryvarden & I. Johans. and related genera from the Neotropics, and *T. luteocontexta* was transferred to *Aegis* Gómez-Mont., Rajchenb. & Robledo according to morphological and molecular data. Recent phylogenetic studies have shown that *Trametopsis* belongs to Irpicaceae Spirin & Zmitr in the phlebioid clade (Justo et al. 2017; Chen et al. 2021). So far, three species are accepted in *Trametopsis*, viz., *T. aborigena*, *T. brasiliensis* and *T. cervina*.

During our investigations of wood-decay fungi, some specimens of the phlebioid clade were collected. These specimens possess glabrous or velutinate to strigose pileal surface, round to angular, irregular, daedaleoid to irpicoid pores, saprophytic on dead wood and causing white rot. Preliminary morphological observations showed that these specimens may belong to *Trametopsis*. To determine the phylogenetic positions of these specimens, we performed phylogenetic analyses of Irpicaceae with emphasis on *Trametopsis* based on the combined sequences datasets of ITS+nLSU and ITS+nLSU+RPB1+RPB2+TEF1. Combining morphological and molecular evidence, two new species, viz., *T. abieticola* and *T. tasmanica* are described and illustrated.

Materials and methods

Morphological studies

The examined specimens were deposited at the herbarium of the Institute of Microbiology, Beijing Forestry University (BJFC). Morphological descriptions and abbreviations used in this study follow Cui et al. (2019) and Song et al. (2021).

Molecular studies and phylogenetic analysis

The procedures for DNA extraction and polymerase chain reaction (PCR) used in this study were the same as described by Liu et al. (2021a) and Sun et al. (2022). The ITS regions were amplified with the primer pairs ITS4 and ITS5, the nLSU regions were amplified with the primer pairs LR0R and LR7, RPB1 was amplified with primer pairs RPB1-Af and RPB1-Cr, RPB2 gene was amplified with the primer pairs fRPB2-f5F and bRPB2-7.1R, and TEF1 gene was amplified with the primer pairs EF1-983F and EF1-1567R (White et al. 1990; Rehner 2001; Matheny et al. 2002; Matheny 2005).

The PCR cycling schedules for different DNA sequences of ITS, nLSU, RPB1, RPB2 and TEF1 genes used in this study followed those used in Liu et al. (2021b, 2022) with some modifications. The PCR products were purified and sequenced at Beijing Genomics Institute, China, with the same primers. All newly generated sequences were submitted to GenBank and were listed in Table 1.

Sequences were aligned with additional sequences downloaded from GenBank (Table 1) using ClustalX (Thompson et al. 1997). Alignment was manually adjusted to allow maximum alignment and to minimise gaps in BioEdit (Hall 1999). Sequence alignment was deposited to TreeBase (https://treebase.org/treebase-web; submission ID 29580). In phylogenetic reconstructions, the sequences of *Phanerochaete albida* Sheng H. Wu and *P. alnea* (Fr.) P. Karst. obtained from GenBank were used as outgroups. The reason for choosing these two species as outgroup taxa is that they belong to *Phanerochaete* in Phanerochaetaceae, and are closely related to Irpicaceae (Chen et al. 2021), which conforms to the outgroup selection rules. Furthermore, species of *Phanerochaete* were also selected as outgroups in other phylogenetic studies of Irpicaceae, such as in El-Gharabawy et al (2021).

Phylogenetic analyses approaches used in this study followed Sun et al. (2020) and Ji et al. (2022). The congruencies of the 2-gene (ITS and nLSU) and 5-gene (ITS, nLSU, RPB1, RPB2 and TEF1) were evaluated with the incongruence length difference (ILD) test (Farris et al. 1994) implemented in PAUP* 4.0b10 (Swofford 2002), under heuristic search and 1000 homogeneity replicates. Maximum parsimony (MP) analysis was performed in PAUP* version 4.0b10 (Swofford 2002). Clade robustness was assessed using a bootstrap (BT) analysis with 1000 replicates (Felsenstein 1985). Descriptive tree statistics tree length (TL), consistency index (CI), retention index (RI), rescaled consistency index (RC), and homoplasy index (HI) were calculated for each Most Parsimonious Tree (MPT) generated. Maximum Likelihood (ML) analysis was performed in RAxML-HPC v. 8.2.3 with a GTR+G+I model (Stamatakis 2014). Bayesian inference (BI) was calculated by MrBayes 3.1.2 (Ronquist and Huelsenbeck 2003) with a general time reversible (GTR) model of DNA substitution and a gamma distribution rate variation across sites determined by MrModeltest 2.3 (Posada and Crandall 1998; Nylander 2008). The branch support was evaluated with a bootstrapping method of 1000 replicates (Hillis and Bull 1993).

Trees were viewed in FigTree v1.4.4 (http://tree.bio.ed.ac.uk/software/figtree/). Branches that received bootstrap supports for maximum parsimony (MP), maximum likelihood (ML) and Bayesian posterior probabilities (BPP) greater than or equal to 75% (MP and ML) and 0.95 (BPP) were considered as significantly supported, respectively.

Table 1. A list of species, specimens, and GenBank accession number of sequences used for phylogenetic analyses in this study.

Species	Sample no.	Locality	GenBank accessions					References
			ITS	nLSU	RPB1	RPB2	TEF1	
Byssomerulius corium	FCUG 2701	Russia	MZ636931	GQ470630	MZ748415	OK136068	MZ913668	Wu et al. (2010); Chen et al. (2021)
B. corium	Wu 1207-55	China	MZ636932	MZ637096	—	—	—	Chen et al. (2021)
B. corium	FP-102382	USA	KP135007	KP135230	KP134802	KP134921	—	Floudas and Hibbett (2015)
Ceriporia bubalinomarginata	Dai 11327	China	JX623953	JX644045	—	—	—	Jia et al. (2014)
C. bubalinomarginata	Dai 12499	China	JX623954	JX644044	—	—	—	Jia et al. (2014)
C. viridans	Spirin 5909	Finland	KX236481	KX236481	—	—	—	Spirin et al. (2016)
C. viridans	Miettinen 11701	Netherlands	KX752600	KX752600	—	—	—	Miettinen et al. (2016)
Crystallicutis cf. *serpens*	Wu 1608-130	China	MZ636946	MZ637108	—	—	—	Chen et al. (2021)
C. cf. *serpens*	Wu 1608-81	China	MZ636947	MZ637109	MZ748435	OK136094	MZ913699	Chen et al. (2021)
C. serpens	HHB-15692	USA	KP135031	KP135200	KP134785	KP134914	—	Floudas and Hibbett (2015)
C. sp.	FP-101245	USA	KP135029	—	—	—	—	Floudas and Hibbett (2015)
Cytidiella albida	GB-1833	Spain	KY948748	KY948889	KY948960	OK136069	MZ913675	Justo et al. (2017); Chen et al. (2021)
C. albomarginata	Wei 18-474	China	MZ636948	MZ637110	MZ748429	OK136070	MZ913678	Chen et al. (2021)
C. albomarginata	Wu 0108-86	China	MZ636949	MZ637111	MZ748430	OK136071	MZ913677	Chen et al. (2021)
C. albomellea	FP-102339	USA	MZ636950	MZ637112	MZ748431	—	—	Chen et al. (2021)
C. nitidula	T-407	USA	KY948747	MZ637113	KY948961	OK136072	MZ913676	Justo et al. (2017); Chen et al. (2021)
Efibula gracilis	FD-455	USA	KP135027	MZ637116	KP134804	OK136077	MZ913679	Floudas and Hibbett (2015); Chen et al. (2021)
E. gracilis	FP-102052	USA	KP135028	—	—	—	—	Floudas and Hibbett (2015)
E. matsuensis	Wu 1011-18	China	MZ636956	MZ637119	MZ748418	OK136078	MZ913680	Chen et al. (2021)
E. matsuensis	Wu 1011-19	China	MZ636957	MZ637120	—	—	—	Chen et al. (2021)
E. tropica	Chen 3596	China	MZ636966	MZ637128	—	—	—	Chen et al. (2021)
E. tropica	Wei 18-149	China	MZ636967	MZ637129	MZ748419	OK136079	MZ913681	Chen et al. (2021)
E. yunnanensis	Wu 880515-1	China	MZ636977	GQ470672	MZ748420	OK136080	MZ913682	Wu et al. (2010); Chen et al. (2021)
E. yunnanensis	Wu 0910-104	China	MZ636976	MZ637138	—	—	—	Chen et al. (2021)
Gloeoporus orientalis	Wei 16-485	China	MZ636980	MZ637141	MZ748443	OK136095	MZ913709	Chen et al. (2021)
G. pannocinctus	L-15726	USA	KP135060	KP135214	KP134867	KP134973	—	Floudas and Hibbett (2015)
Irpex flavus	Wu 0705-1	China	MZ636988	MZ637149	MZ748432	OK136087	MZ913683	Chen et al. (2021)
I. flavus	Wu 0705-2	China	MZ636989	MZ637150	—	—	—	Chen et al. (2021)
I. hacksungii	F 2008	South Korea	FJ750851	—	—	—	—	Lee et al. (2008)
I. hydnoides	KUC 20121109-01	South Korea	KJ668510	KJ668362	—	—	—	Jang et al. (2016)
I. laceratus	WHC 1372	China	MZ636990	MZ637151	—	—	—	Chen et al. (2021)

Species	Sample no.	Locality	GenBank accessions					References
			ITS	nLSU	RPB1	RPB2	TEF1	
I. lacteus	DO 421	Sweden	JX109852	JX109852	—	JX109882	—	Binder et al. (2013)
I. lacteus	FD-93	USA	KP135025	—	—	—	—	Floudas and Hibbett (2015)
I. latemarginatus	FP-55521-T	USA	KP135024	KP135202	KP134805	KP134915	—	Floudas and Hibbett (2015)
I. latemarginatus	Dai 7165	China	KY131834	KY131893	—	—	—	Wu et al. (2017)
I. lenis	Wu 1608-14	China	MZ636991	MZ637152	MZ748434	—	MZ913685	Chen et al. (2021)
I. lenis	Wu 1608-22	China	MZ636992	MZ637153	—	—	—	Chen et al. (2021)
I. rosettiformis	LR40855	USA	JN649347	JN649347	—	—	—	Sjökvist et al. (2012)
I. rosettiformis	Meijer3729	Brazil	JN649346	JN649346	—	JX109875	JX109904	Sjökvist et al. (2012); Binder et al. (2013)
Leptoporus mollis	LE BIN 3849	Russia	MG735341	—	—	—	—	Psurtseva (2010)
L. mollis	RLG-7163	USA	KY948794	MZ637155	KY948956	OK136101	MZ913693	Justo et al. (2017); Chen et al. (2021)
Meruliopsis albostramineus	HHB 10729	USA	KP135051	KP135229	KP134787	—	—	Floudas and Hibbett (2015)
M. crassitunicata	CHWC 1506-46	China	LC427010	LC427034	—	—	—	Chen et al. (2020)
M. leptocystidiata	Wu 1708-43	China	LC427013	LC427033	LC427070	—	—	Chen et al. (2020)
M. parvispora	Wu 1209-58	China	LC427017	LC427039	LC427065	—	—	Chen et al. (2020)
M. taxicola	GC 1704-60	China	LC427028	LC427050	LC427063	—	—	Chen et al. (2020)
Phanerochaete albida	GC 1407-14	China	MZ422788	MZ637179	MZ748384	OK136013	MZ913704	Chen et al. (2021)
P. alnea	FP-151125	USA	KP135177	MZ637181	MZ748385	OK136014	MZ913641	Floudas and Hibbett (2015); Chen et al. (2021)
Phanerochaetella angustocystidiata	Wu 9606-39	China	MZ637020	GQ470638	MZ748422	OK136082	MZ913687	Wu et al. (2010); Chen et al. (2021)
P. angustocystidiata	GC 1501-20	China	MZ637017	MZ637225	—	—	—	Chen et al. (2021)
P. exilis	HHB-6988	USA	KP135001	KP135236	KP134799	KP134918	—	Floudas and Hibbett (2015)
P. formosana	Chen 479	China	MZ637023	GQ470650	MZ748424	OK136084	MZ913718	Wu et al. (2010); Chen et al. (2021)
P. formosana	Chen 3468	China	MZ637022	MZ637229	—	—	—	Chen et al. (2021)
P. leptoderma	Chen 1362	China	MZ637025	GQ470646	MZ748423	OK136083	MZ913689	Wu et al. (2010); Chen et al. (2021)
P. leptoderma	Wu 1703-9	China	MZ637027	MZ637232	—	—	—	Wu et al. (2010)
P. xerophila	HHB-8509	USA	KP134996	KP135259	KP134800	KP134919	MZ913688	Floudas and Hibbett (2015); Chen et al. (2021)
P. xerophila	KKN-172	USA	KP134997	—	—	—	—	Floudas and Hibbett (2015)
Raduliporus aneirinus	HHB-15629	USA	KP135023	KP135207	KP134795	—	—	Floudas and Hibbett (2015)
R. aneirinus	Wu 0409-199	China	MZ637068	MZ637267	—	OK136096	MZ913712	Chen et al. (2021)
R. pseudogilvescens	Wu 9508-54	China	MZ637069	MZ637269	—	—	—	Chen et al. (2021)
Resiniporus pseudogilvescens	Wu 1209-46	China	KY688203	MZ637268	MZ748436	OK136097	MZ913713	Chen et al. (2018); Chen et al. (2021)
R. resinascens	BRNM 710169	Czech Republic	FJ496675	FJ496698	—	—	—	Tomšovský et al. (2010)
Trametopsis abieticola	**Cui 18363**	**China**	**ON041038**	**ON041054**	**ON099403**	**ON099411**	**ON083777**	**Present study**
T. abieticola	**Cui 18383**	**China**	**ON041039**	**ON041055**	**ON099404**	**ON099412**	**ON083778**	**Present study**

Species	Sample no.	Locality	GenBank accessions					References
			ITS	nLSU	RPB1	RPB2	TEF1	
T. aborigena	Robledo 1236	Argentina	KY655336	KY655338	—	—	—	Gómez-Montoya et al. (2017)
T. aborigena	Robledo 1238	Argentina	KY655337	KY655339	—	—	—	Gómez-Montoya et al. (2017)
T. brasiliensis	Meijer 3637	Brazil	JN710510	JN710510	—	—	—	Miettinena et al. (2012)
T. cervina	**Cui 17712**	**China**	**ON041040**	**ON041056**	—	**ON099413**	**ON083779**	**Present study**
T. cervina	**Cui 18017**	**China**	**ON041041**	**ON041057**	—	**ON099414**	**ON083780**	**Present study**
T. cervina	**Cui 18019**	**China**	**ON041042**	**ON041058**	**ON099405**	**ON099415**	**ON083781**	**Present study**
T. cervina	**Dai 21818**	**China**	**ON041043**	**ON041059**	**ON099406**	—	**ON083782**	**Present study**
T. cervina	**Dai 21820**	**China**	**ON041044**	**ON041060**	**ON099407**	**ON099416**	**ON083783**	**Present study**
T. cervina	**Dai 22804**	**China**	**ON041045**	**ON041061**	—	**ON099417**	**ON083784**	**Present study**
T. cervina	**Dai 23454**	**China**	**ON041046**	**ON041062**	—	—	**ON083785**	**Present study**
T. cervina	**He 6863**	**China**	**ON041047**	**ON041063**	**ON099408**	**ON099418**	**ON083786**	**Present study**
T. cervina	MG 299	Iran	KU213592	KU213594	—	—	—	—
T. cervina	TJV-93-216T	USA	JN165020	JN164796	JN164839	JN164877	JN164882	Justo and Hibbett (2011)
T. tasmanica	**Cui 16606**	**Australia**	**ON041048**	**ON041064**	**ON099409**	**ON099419**	**ON083787**	**Present study**
T. tasmanica	**Cui 16607**	**Australia**	**ON041049**	**ON041065**	**ON099410**	**ON099420**	**ON083788**	**Present study**

Newly generated sequences for this study are shown in bold.

Results

Phylogeny

The combined 2-gene (ITS+nLSU) sequences dataset had an aligned length of 1893 characters, including gaps (619 characters for ITS, 1274 characters for nLSU), of which 1307 characters were constant, 105 were variable and parsimony-uninformative, and 481 were parsimony-informative. MP analysis yielded 26 equally parsimonious trees (TL = 2150, CI = 0.409, RI = 0.776, RC = 0.317, HI = 0.591). The best-fit evolutionary models applied in Bayesian analyses were selected by MrModeltest2 v. 2.3 for each region of the two genes, the model for ITS was GTR+I+G with equal frequency of nucleotides, while the model for nLSU was SYM+I+G with equal frequency of nucleotides. ML analysis resulted in a similar topology as MP and Bayesian analyses, and only the ML topology is shown in Fig. 1.

The combined 5-gene (ITS+nLSU+RPB1+RPB2+TEF1) sequences dataset had an aligned length of 4609 characters, including gaps (619 characters for ITS, 1274 characters for nLSU, 1170 characters for RPB1, 1001 characters for RPB2, 545 characters for TEF1), of which 2675 characters were constant, 272 were variable and parsimony-uninformative, and 1662 were parsimony-informative. MP analysis yielded 36 equally parsimonious trees (TL = 9247, CI = 0.362, RI = 0.652, RC = 0.236, HI = 0.638). The best-fit evolutionary models applied in Bayesian analyses were selected by MrModeltest2 v. 2.3 for each region of the two genes, the model for ITS, RPB1, RPB2 and TEF1was GTR+I+G with equal frequency of nucleotides, while the model for nLSU was SYM+I+G with equal frequency of nucleotides. ML analysis resulted in a similar topology as MP and Bayesian analyses, and only the ML topology is shown in Fig. 2.

Thephylogenetictreesinferredfrom ITS+nLSUandITS+nLSU+RPB1+RPB2+TEF1 gene sequences were all obtained from 78 fungal samples representing 42 taxa of Irpicaceae and two taxa of Phanerochaetaceae within the phlebioid clade (Figs 1, 2). Phylogenetic analyses showed that *Trametopsis abieticola*, *T. aborigena*, *T. brasiliensis*, *T. cervina* and *T. tasmanica* grouped together within *Trametopsis* by high support (100% ML, 100% MP, 1.00 BPP; Figs 1, 2).

Taxonomy

Trametopsis abieticola **B.K. Cui & Shun Liu, sp. nov.**
MycoBank No: 844097
Figs 3, 4

Diagnosis. *Trametopsis abieticola* is distinguished from *T. tasmanica* by larger pores (0.5–1 per mm) and basidiospores (5.8–7.2 × 1.9–2.6 μm), and by being distributed in the high altitude of mountains and growing on *Abies* sp.

Holotype. China. Xizang Autonomous Region (Tibet), Mangkang County, Mangkang Mountain, on fallen trunk of *Abies* sp., 8 September 2020, Cui 18383 (holotype BJFC 035242).

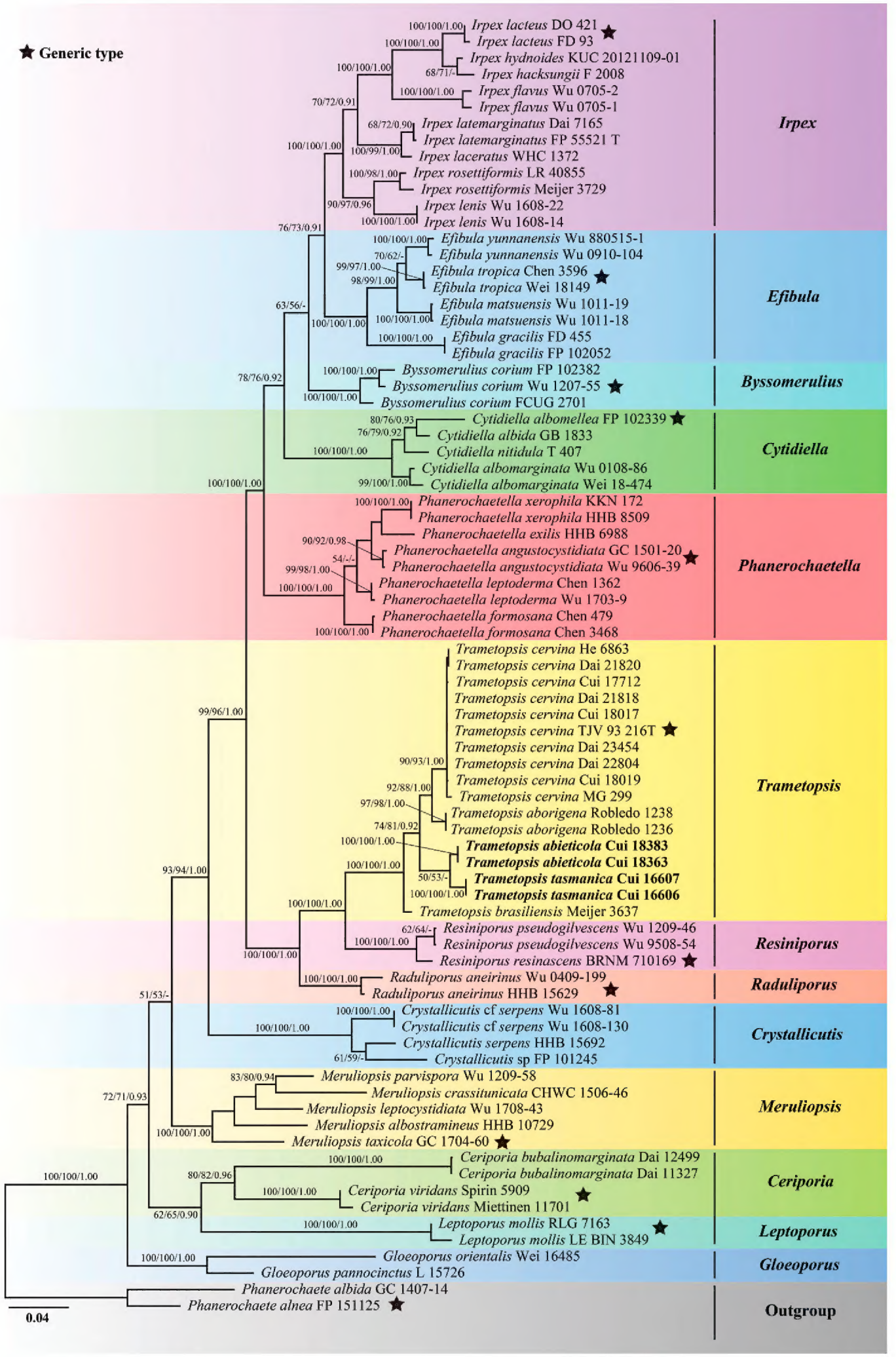

Figure 1. Maximum likelihood tree illustrating the phylogeny of *Trametopsis* based on the combined sequences dataset of ITS+nLSU. Branches are labelled with maximum likelihood bootstrap higher than 50%, parsimony bootstrap proportions higher than 50% and Bayesian posterior probabilities more than 0.90 respectively. Bold names = New species.

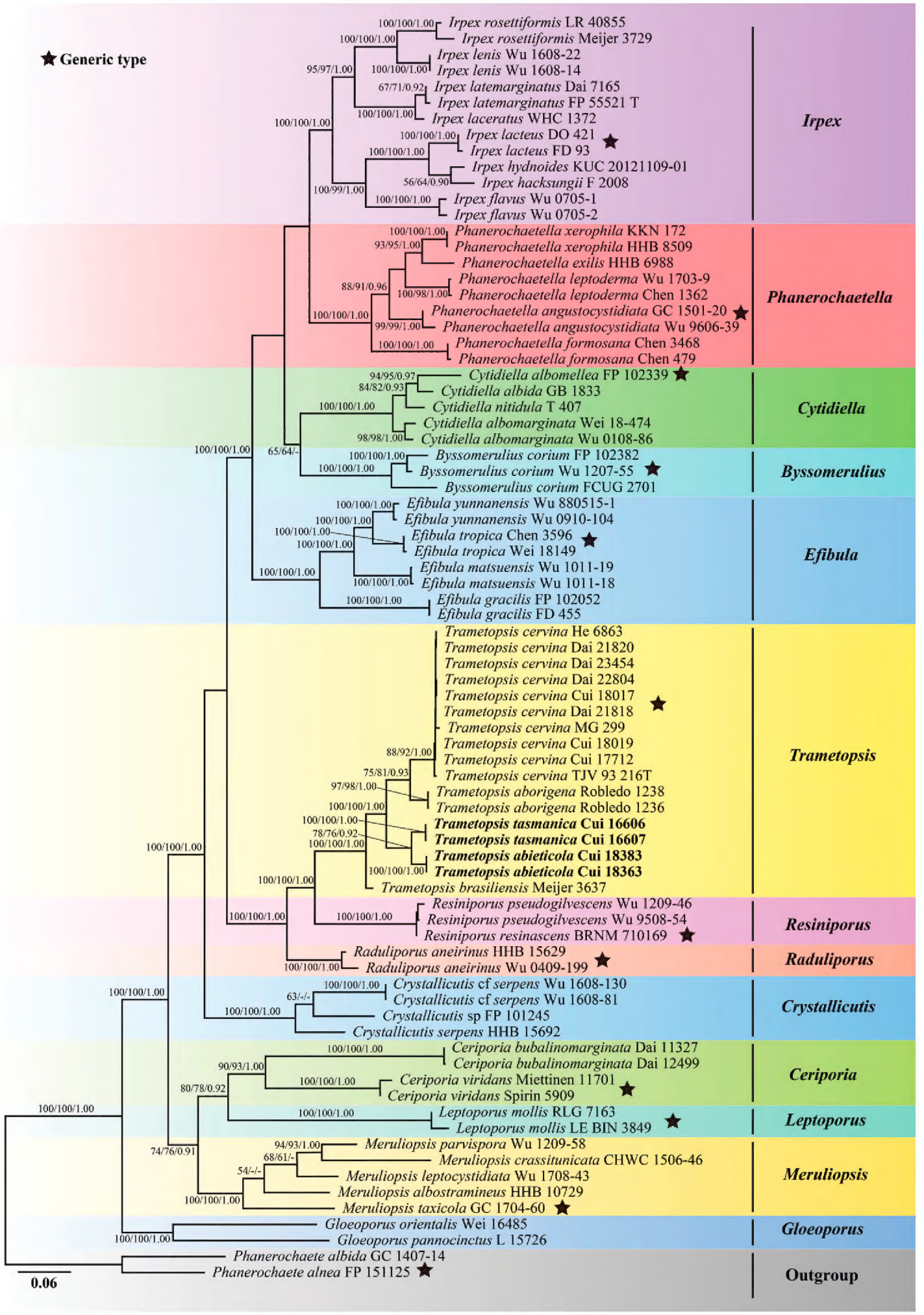

Figure 2. Maximum likelihood tree illustrating the phylogeny of *Trametopsis* based on the combined sequences dataset of ITS+nLSU+RPB1+RPB2+TEF1. Branches are labelled with maximum likelihood bootstrap higher than 50%, parsimony bootstrap proportions higher than 50% and Bayesian posterior probabilities more than 0.90 respectively. Bold names = New species.

Figure 3. Basidiomata of *Trametopsis abieticola* (Holotype, Cui 18383). Scale bar: 3 cm.

Etymology. *Abieticola* (Lat.): referring to the species grows on *Abies* sp.

Fruiting body. Basidiomata annual, pileate, solitary or imbricate, soft corky to corky, without odour or taste when fresh, becoming corky and light in weight upon drying. Pilei applanate to flabelliform, projecting up to 9.5 cm long, 5.5 cm wide, and

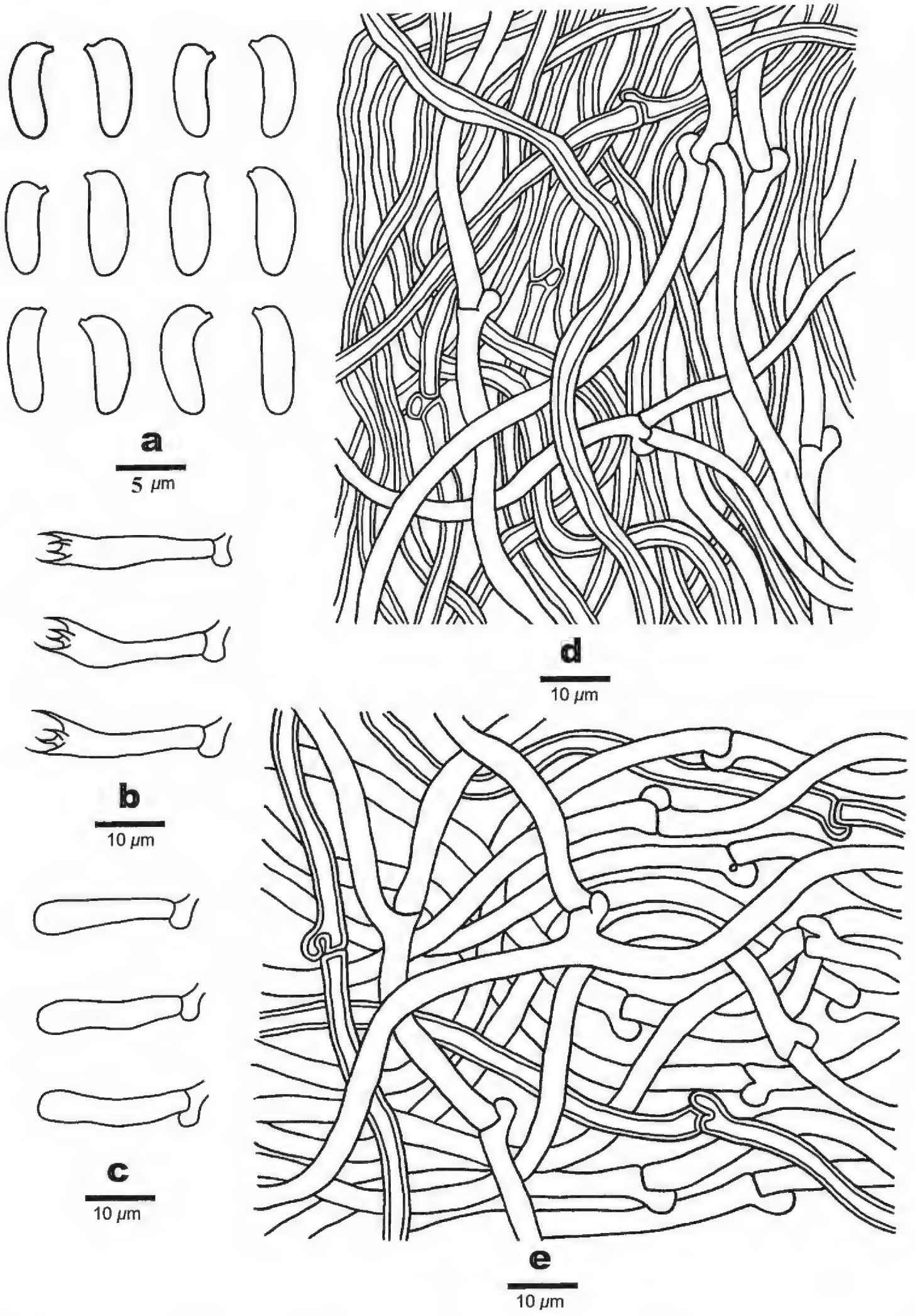

Figure 4. Microscopic structures of *Trametopsis abieticola* (Holotype, Cui 18383) **a** basidiospores **b** basidia **c** basidioles **d** hyphae from trama **e** hyphae from context.

2 cm thick at base. Pileal surface buff to buff-yellow when fresh, becoming pinkish buff to clay-buff when dry, strigose or glabrous; margin white to cream when fresh, becoming cream to buff-yellow when dry, obtuse to acute. Pore surface cream to buff when fresh, becoming pinkish buff to greyish brown upon drying; pores round to angular, 0.5–1 per mm; dissepiments slightly thick, entire to lacerate. Context corky, cream to buff yellow, up to 8 mm thick. Tubes concolorous with pore surface, corky, up to 7 mm long.

Hyphal structure. Hyphal system monomitic in context, dimitic in trama; generative hyphae with clamp connections; skeletal hyphae IKI–, CB–; tissues unchanged in KOH.

Context. Generative hyphae hyaline, thin- to slightly thick-walled, occasionally branched, loosely interwoven, 2.8–4.2 μm in diam.

Tubes. Generative hyphae frequent, hyaline, thin- to slightly thick-walled, occasionally branched, 1.8–3.5 μm in diam.; skeletal hyphae dominant, hyaline, thick-walled with a wide to narrow lumen, occasionally branched, more or less straight, interwoven, 2–4.5 μm in diam. Cystidia and cystidioles absent. Basidia clavate, bearing four sterigmata and a basal clamp connection, 17.8–22.5 × 4.3–5.5 μm; basidioles dominant, similar to basidia but smaller.

Spores. Basidiospores cylindrical, hyaline, thin-walled, smooth, IKI–, CB–, (5.7–)5.8–7.2 × (1.8–)1.9–2.6(–2.8) μm, L = 6.57 μm, W = 2.22 μm, Q = 2.75–3.26 (n = 60/2).

Type of rot. White rot.

Additional specimen (paratype) examined. China. Sichuan Province, Yajiang County, Kangbahanzi Village, on fallen trunk of *Abies* sp., 7 September 2020, Cui 18363 (BJFC 035222).

Trametopsis tasmanica **B.K. Cui & Shun Liu, sp. nov.**

MycoBank No: 844098

Figs 5, 6

Diagnosis. *Trametopsis tasmanica* is distinguished from *T. abieticola* by resupinate basidiomata, smaller pores (2–4 per mm) and basidiospores (5.2–6.3 × 1.8–2.2 μm), and by growing on *Eucalyptus* sp.

Holotype. Australia. Tasmania, Hobart, Mount Wellington, on rotten wood of *Eucalyptus* sp., 13 May 2018, Cui 16606 (holotype BJFC 029905).

Etymology. *Tasmanica* (Lat.): referring to the species collected from Tasmania in Australia.

Fruiting body. Basidiomata annual, resupinate, not easily separated from the substrate, without odour or taste when fresh, becoming corky to fragile and light in weight upon drying; up to 5.5 cm long, 2 cm wide, and 7 mm thick at centre. Pore surface cream to pinkish-buff when fresh, becoming honey-yellow to snuff brown upon drying; pores round to angular, 2–4 per mm; dissepiments slightly thick, entire to lacerate. Context very thin, corky, cream to buff, up to 2 mm thick. Tubes concolorous with pore surface, corky, up to 4 mm long.

Figure 5. *Trametopsis tasmanica* (Holotype, Cui 16606 and paratype, Cui 16607). Scale bar: 1 cm.

Hyphal structure. Hyphal system monomitic in context, dimitic in trama; generative hyphae with clamp connections; skeletal hyphae IKI–, CB–; tissues unchanged in KOH.

Context. Generative hyphae hyaline, thin- to slightly thick-walled with a wide lumen, occasionally branched, loosely interwoven, 2.7–4 μm in diam.

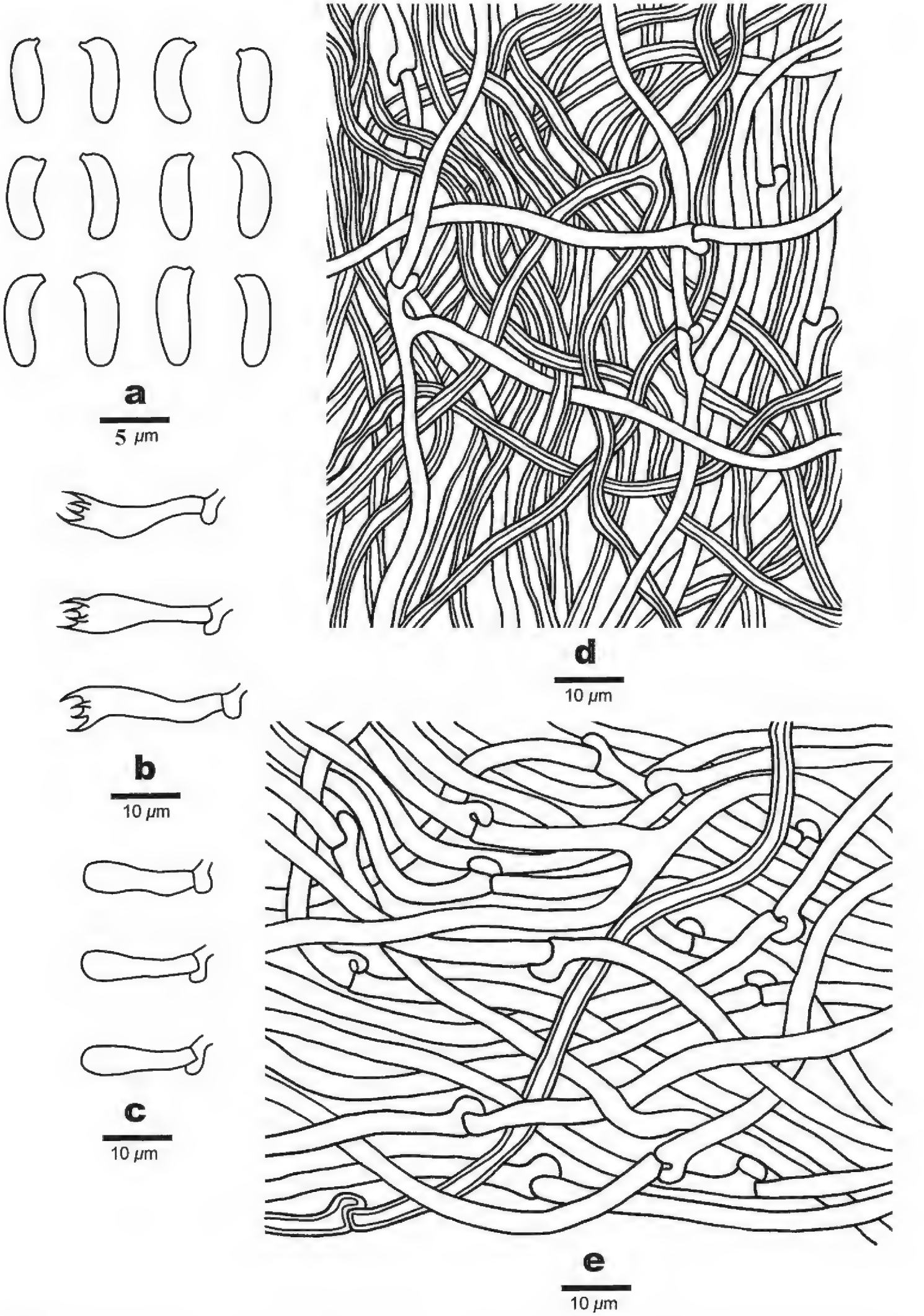

Figure 6. Microscopic structures of *Trametopsis tasmanica* (Holotype, Cui 16606) **a** Basidiospores **b** Basidia **c** Basidioles **d** Hyphae from trama **e** Hyphae from context.

Tubes. Generative hyphae frequent, hyaline, thin-walled, occasionally branched, 2–3 μm in diam.; skeletal hyphae dominant, hyaline, thick-walled with a wide to narrow lumen, occasionally branched, more or less straight, interwoven, 2–3.7 μm in diam. Cystidia and cystidioles absent. Basidia clavate, bearing four sterigmata and a basal clamp connection, 16–19.5 × 3.7–5 μm; basidioles dominant, similar to basidia but smaller.

Spores. Basidiospores cylindrical, hyaline, thin-walled, smooth, IKI–, CB–, (5–)5.2–6.3 × (1.7–)1.8–2.2(–2.4) μm, L = 5.84 μm, W = 2.02 μm, Q = 2.66–3.13 (n = 60/2).

Type of rot. White rot.

Additional specimen (paratype) examined. Australia. Tasmania, Hobart, Mount Wellington, on rotten branch of *Eucalyptus* sp., 13 May 2018, Cui 16607 (BJFC 029906).

Discussion

In this study, the phylogenetic analyses of *Trametopsis* and related genera are inferred from the combined datasets of ITS+nLSU sequences (Fig. 1) and ITS+nLSU+RPB1+RPB2+TEF1 sequences (Fig. 2). The genera; *Raduliporus* Spirin & Zmitr., *Resiniporus* Zmitr. and *Trametopsis* grouped together and formed a highly supported lineage (Figs 1 and 2), which was called the *Trametopsis* lineage by Chen et al. (2021). Morphologically, *Raduliporus* and *Resiniporus* differ from *Trametopsis* by having a monomitic hyphal system and ellipsoid basidiospores (Chen et al. 2021). Phylogenetically, *T. abieticola* and *T. tasmanica* clustered with other *Trametopsis* species (Figs 1, 2) with high supports (100% MP, 100% ML, 1.00 BPP; Figs 1, 2). The main morphological characters and ecological habits of species in *Trametopsis* are provided in Table 2. The geographical locations of the *Trametopsis* species distributed in the world are indicated on the map (Fig. 7).

Trametopsis abieticola is distributed in high altitude areas of the Hengduan Mountains (altitude > 3500 m) and grows on *Abies* sp. In the phylogenetic trees, *T. abieticola* is closely related to *T. tasmanica* (Figs 1, 2). Morphologically, *T. tasmanica* differs from *T. abieticola* in having resupinate basidiomata, smaller pores (2–4 per mm) and basidiospores (5.2–6.3 × 1.8–2.2 μm), being distributed in Australia and growing on *Eucalyptus* sp. *Trametopsis cervina* can also distributed in high altitude areas of the Hengduan Mountains (according to our investigations), but *T. cervina* differs from *T. abieticola* by its smaller pores (2–4 per mm), longer basidiospores (6–9 × 2–3 μm; Tomšovský 2008), and usually growing on angiosperm trees. *Trametopsis aborigena*, *T. brasiliensis* and *T. abieticola* share an annual growth habit, a monomitic hyphal system in context, dimitic in trama and clamped generative hyphae; but *T. aborigena* differs from *T. abieticola* by having light pale brown to pale yellowish pileal surface with yellowish red to dark yellowish brown radial veins, smaller pores (1–3 per mm) and basidiospores (5–7 × 1–2 μm), and being distributed in neotropical regions of Argentina

Table 2. The main morphological characters and ecological habits of species in *Trametopsis*. New species are shown in bold.

Species name	Distribution	Climate zone	Host	Fruiting body	Pores (per mm)	Basidia (μm)	Basidiospores (μm)	References
Trametopsis abieticola	**Asia (China)**	**Alpine plateau**	**Gymnosperm (*Abies*)**	**Pileate**	**0.5–1**	**17.8–22.5 × 4.3–5.5**	**5.8–7.2 × 1.9–2.6**	**Present study**
T. aborigena	South America (Argentina)	Neotropical	Angiosperm (Undetermined)	Pileate, effused-reflexed or occasionally resupinate	1–3	19–22 × 5–6	5–7 × 1–2.5	Gómez-Montoya et al. (2017)
T. brasiliensis	South America (Brazil)	Neotropical	Angiosperm (*Dicotyledonous*)	Pileate	1–2	15–20 × 4–5	4.5–5.5 × 1.8–2.2	Ryvarden and Meijer (2002); Gómez-Montoya et al. (2017)
T. cervina	Africa (Burundi, Rwanda, Tanzania), Asia (China, Iran), Europe (Austria, Belgium, Czech, France, Greece, Italy, Slovakia, Poland, Ukraine, Russia, etc.), and North America (Canada, USA)	Alpine plateau, temperate to tropical	Angiosperm (*Acer*, *Alnus*, *Betula*, *Carpinus*, *Elaeocarpus*, *Fagus*, *Juglans*, *Liquidambar*, *Populus*, *Quercus*, *Salix*, etc.); Gymnosperm (*Larix*, *Pinus*)	Effused-reflexed to pileate or occasionally resupinate	2–4	20–25 × 5–7	6–9 × 2–3	Tomšovský (2008); Gómez-Montoya et al. (2017); present study
T. tasmanica	**Oceania (Australia)**	**Temperate marine climate**	**Angiosperm (*Eucalyptus*)**	**Resupinate**	**2–4**	**16–19.5 × 3.7–5**	**5.2–6.3 × 1.8–2.2**	**Present study**

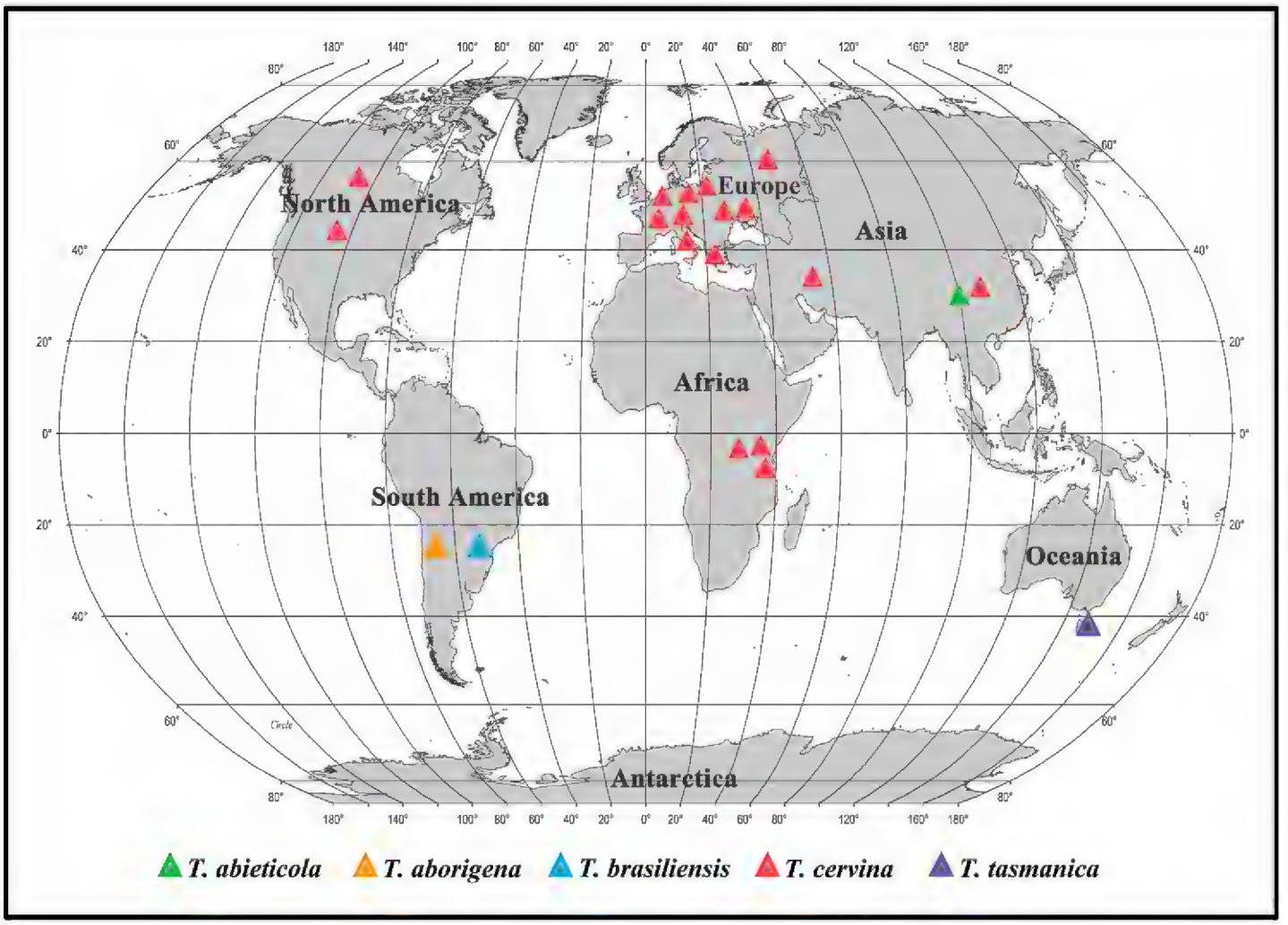

Figure 7. The geographical locations of the *Trametopsis* species distributed in the world.

(Gómez-Montoya et al. 2017); *T. brasiliensis* differs from *T. abieticola* in having smaller pores (1–2 per mm) and basidiospores (4.5–5.5 × 1.8–2.2 μm), and being distributed in neotropical regions of Brazil (Gómez-Montoya et al. 2017).

Trametopsis tasmanica is distributed in Tasmania, Australia and grows on *Eucalyptus* sp. Before that, there was no report of *Trametopsis* in Oceania. Morphologically, *T. tasmanica* and *T. cervina* share similar-sized pores, but *T. cervina* differs from *T. tasmanica* by its pileate to effused-reflexed basidiomata, larger basidiospores (6–9 × 2–3 μm; Tomšovský 2008). *Trametopsis aborigena*, *T. brasiliensis* and *T. tasmanica* are only distributed in the southern hemisphere and grow on angiosperm trees. However, *T. aborigena* differs from *T. tasmanica* by having pileate, effused-reflexed to occasionally resupinate basidiomata, larger basidia (19–22 × 5–6 μm) and basidiospores (5–7 × 1–2.5 μm), and being distributed in neotropical regions of Argentina (Gómez-Montoya et al. 2017); *T. brasiliensis* differs from *T. tasmanica* in having pileate basidiomata, larger pores (1–2 per mm) and distributed in neotropical regions of Brazil (Gómez-Montoya et al. 2017).

In summary, we performed a taxonomic and phylogenetic study of *Trametopsis*. The concepts and species number of the *Trametopsis* are updated. So far, five species are accepted in the *Trametopsis* around the world. Currently, *Trametopsis* is characterised by an annual growth habit, effused-reflexed to pileate or resupinate, solitary or imbricate basidiomata, pinkish buff to cinnamon or clay-buff, zonate or azonate, glabrous or

velutinate to strigose pileal surface, cream, pale yellow to greyish brown pore surface with round to angular, irregular, daedaleoid to irpicoid pores, a monomitic hyphal system in context, dimitic in trama, clamped generative hyphae, and allantoid to cylindrical basidiospores; it grows on different angiosperm and gymnosperm trees, causing white rot of wood (Tomšovský 2008; Gómez-Montoya et al. 2017).

Acknowledgements

We express our gratitude to Ms. Xing Ji (China) for help during field collections and molecular studies. Also to Drs. Genevieve Gates (Australia), Xiao-Lan He (China) and Hai-Xia Ma (China) for their assistance during field collections. The research is supported by the National Natural Science Foundation of China (Nos. 31870008, U2003211, 31900017), Beijing Forestry University Outstanding Young Talent Cultivation Project (No. 2019JQ03016).

References

Binder M, Justo A, Riley R, Salamov A, López-Giráldez F, Sjökvist E, Copeland A, Foster B, Sun H, Larsson E, Larsson KH, Townsend J, Grigoriev IV, Hibbett DS (2013) Phylogenetic and phylogenomic overview of the Polyporales. Mycologia 105(6): 1350–1373. https://doi.org/10.3852/13-003

Chen CC, Wu SH, Chen CY (2018) Four species of polyporoid fungi newly recorded from Taiwan. Mycotaxon 133(1): 45–54. https://doi.org/10.5248/133.45

Chen CC, Chen CY, Lim YW, Wu SH (2020) Phylogeny and taxonomy of *Ceriporia* and other related taxa and description of three new species. Mycologia 112(1): 64–82. https://doi.org/10.1080/00275514.2019.1664097

Chen CC, Chen CY, Wu SH (2021) Species diversity, taxonomy and multi-gene phylogeny of phlebioid clade (Phanerochaetaceae, Irpicaceae, Meruliaceae) of Polyporales. Fungal Diversity 6(1): 337–442. https://doi.org/10.1007/s13225-021-00490-w

Cui BK, Li HJ, Ji X, Zhou JL, Song J, Si J, Yang ZL, Dai YC (2019) Species diversity, taxonomy and phylogeny of Polyporaceae (Basidiomycota) in China. Fungal Diversity 97(1): 137–392. https://doi.org/10.1007/s13225-019-00427-4

El-Gharabawy HM, Leal-Dutra CA, Griffith GW (2021) *Crystallicutis* gen. nov. (Irpicaceae, Basidiomycota), including *C. damiettensis* sp. nov., found on *Phoenix dactylifera* (date palm) trunks in the Nile Delta of Egypt. Fungal Biology 125(6): 447–458. https://doi.org/10.1016/j.funbio.2021.01.004

Farris JS, Källersjö M, Kluge AG, Kluge AG, Bult C (1994) Testing significance of incongruence. Cladistics 10(3): 315–319. https://doi.org/10.1111/j.1096-0031.1994.tb00181.x

Felsenstein J (1985) Confidence intervals on phylogenies: An approach using the bootstrap. Evolution; International Journal of Organic Evolution 39(4): 783–791. https://doi.org/10.1111/j.1558-5646.1985.tb00420.x

Floudas D, Hibbett DS (2015) Revisiting the taxonomy of *Phanerochaete* (Polyporales, Basidiomycota) using a four gene dataset and extensive ITS sampling. Fungal Biology 119(8): 679–719. https://doi.org/10.1016/j.funbio.2015.04.003

Gómez-Montoya N, Drechsler-Santos ER, Ferreira-Lopes V, Tomšovský M, Urcelay C, Robledo GL (2017) New insights on *Trametopsis* Tomšovský (Polyporales Gäum.) based on phylogenetic evidences and morphological analyses of neotropical species. Phytotaxa 311(2): 155–166. https://doi.org/10.11646/phytotaxa.311.2.3

Hall TA (1999) Bioedit: A user-friendly biological sequence alignment editor and analysis program for Windows 95/98/NT. Nucleic Acids Symposium Series 41: 95–98.

Hillis DM, Bull JJ (1993) An empirical test of bootstrapping as a method for assessing confidence in phylogenetic analysis. Systematics and Biodiversity 42: 182–192. https://doi.org/10.1093/sysbio/42.2.182

Jang Y, Jang S, Lee J, Lee H, Lim YW, Kim C, Kim JJ (2016) Diversity of wood-inhabiting polyporoid and corticioid fungi in Odaesan National Park, Korea. Mycobiology 44(4): 217–236. https://doi.org/10.5941/MYCO.2016.44.4.217

Ji X, Zhou JL, Song CG, Xu TM, Wu DM, Cui BK (2022) Taxonomy, phylogeny and divergence times of *Polyporus* (Basidiomycota) and related genera. Mycosphere: Journal of Fungal Biology 13: 1–52. https://doi.org/10.5943/mycosphere/13/1/1

Jia BS, Zhou LW, Cui BK, Rivoire B, Dai YC (2014) Taxonomy and phylogeny of *Ceriporia* (Polyporales, Basidiomycota) with an emphasis of Chinese collections. Mycological Progress 13(1): 81–93. https://doi.org/10.1007/s11557-013-0895-5

Justo A, Hibbett DS (2011) Phylogenetic classification of *Trametes* (Basidiomycota, Polyporales) based on a five-marker dataset. Taxon 60(6): 1567–1583. https://doi.org/10.1002/tax.606003

Justo A, Miettinen O, Floudas D, Ortiz-Santana B, Sjökvist E, Lindner D, Nakason K, Niemelä T, Larsson K-H, Ryvarden L, Hibbett DS (2017) A revised family-level classification of the Polyporales (Basidiomycota). Fungal Biology 121(9): 798–824. https://doi.org/10.1016/j.funbio.2017.05.010

Lee JS, Kim C, Lim YW (2008) *Irpex hacksungii* sp. nov. (Polyporaceae) from Korea. Mycotaxon 106: 423–429.

Liu S, Han ML, Xu TM, Wang Y, Wu DM, Cui BK (2021a) Taxonomy and phylogeny of the *Fomitopsis pinicola* complex with descriptions of six new species from east Asia. Frontiers in Microbiology 12: e644979. https://doi.org/10.3389/fmicb.2021.644979

Liu S, Shen LL, Wang Y, Xu TM, Gates G, Cui BK (2021b) Species diversity and molecular phylogeny of *Cyanosporus* (Polyporales, Basidiomycota). Frontiers in Microbiology 12: 631166. https://doi.org/10.3389/fmicb.2021.631166

Liu S, Xu TM, Song CG, Zhao CL, Wu DM, Cui BK (2022) Species diversity, molecular phylogeny and ecological habits of *Cyanosporus* (Polyporales, Basidiomycota) with an emphasis on Chinese collections. MycoKeys 86: 19–46. https://doi.org/10.3897/mycokeys.86.78305

Matheny PB (2005) Improving phylogenetic inference of mushrooms with RPB1 and RPB2 nucleotide sequences (*Inocybe*, Agaricales). Molecular Phylogenetics and Evolution 35(1): 1–20. https://doi.org/10.1016/j.ympev.2004.11.014

Matheny PB, Liu YJ, Ammirati JF, Hall BD (2002) Using RPB1 sequences to improve phylogenetic inference among mushrooms (*Inocybe*, Agaricales). American Journal of Botany 89(4): 688–698. https://doi.org/10.3732/ajb.89.4.688

Miettinen O, Spirin V, Vlasák J, Rivoire B, Stenroos S, Hibbett D (2016) Polypores and genus concepts in Phanerochaetaceae (Polyporales, Basidiomycota). MycoKeys 17: 1–46. https://doi.org/10.3897/mycokeys.17.10153

Miettinena O, Larssonb E, Sjökvist E, Larssonc KH (2012) Comprehensive taxon sampling reveals unaccounted diversity and morphological plasticity in a group of dimitic polypores (Polyporales, Basidiomycota). Cladistics 28(3): 251–270. https://doi.org/10.1111/j.1096-0031.2011.00380.x

Nylander JAA (2008) MrModeltest2 v. 2.3. Evolutionary Biology Centre, Uppsala University, Program distributed by the author.

Posada D, Crandall KA (1998) Modeltest: Testing the model of DNA substitution. Bioinformatics (Oxford, England) 14(9): 817–818. https://doi.org/10.1093/bioinformatics/14.9.817

Psurtseva NV (2010) Conservation of medicinal mushrooms in the V. L. Komarov Botanical Institute Basidiomycetes Culture Collection (LE-BIN, Russia). International Journal of Medicinal Mushrooms 12(2): 193–199. https://doi.org/10.1615/IntJMedMushr.v12.i2.100

Rehner S (2001) Primers for Elongation Factor 1-a (EF1-a). http://ocid.nacse.org/research/deephyphae/EF1primer.pdf

Ronquist F, Huelsenbeck JP (2003) MRBAYES 3: Bayesian phylogenetic inference under mixed models. Bioinformatics (Oxford, England) 19(12): 1572–1574. https://doi.org/10.1093/bioinformatics/btg180

Ryvarden L, Meijer AAR (2002) Studies in neotropical polypores 14. New species from the state of Paraná, Brazil. Synopsis Fungorum 15: 34–69.

Sjökvist E, Larsson E, Eberhardt U, Ryvarden L, Larsson KH (2012) Stipitate stereoid basidiocarps have evolved multiple times. Mycologia 104(5): 1046–1055. https://doi.org/10.3852/11-174

Song CG, Ji X, Liu S, He XL, Cui BK (2021) Taxonomy and molecular phylogeny of *Phellodon* (Thelephorales) with descriptions of four new species from Southwest China. Forests 12(7): e932. https://doi.org/10.3390/f12070932

Spirin V, Vlasák J, Rivoire B, Kout J, Kotiranta H, Miettinen O (2016) Studies in the *Ceriporia purpurea* group (Polyporales, Basidiomycota), with notes on similar *Ceriporia* species. Cryptogamie. Mycologie 37(4): 421–435. https://doi.org/10.7872/crym/v37.iss4.2016.421

Stamatakis A (2014) RAxML Version 8: A tool for phylogenetic analyses and post analyses of large phylogenies. Bioinformatics (Oxford, England) 30(9): 1312–1313. https://doi.org/10.1093/bioinformatics/btu033

Sun YF, Costa-Rezende DH, Xing JH, Zhou JL, Zhang B, Gibertoni TB, Gates G, Glen M, Dai YC, Cui BK (2020) Multi-gene phylogeny and taxonomy of *Amauroderma* s. lat. (Ganodermataceae). Persoonia 44(1): 206–239. https://doi.org/10.3767/persoonia.2020.44.08

Sun YF, Xing JH, He XL, Wu DM, Song CG, Liu S, Vlasák J, Gates G, Gibertoni TB, Cui BK (2022) Species diversity, systematic revision and molecular phylogeny of Ganodermataceae

(Polyporales, Basidiomycota) with an emphasis on Chinese collections. Studies in Mycology 101: 287–415. https://doi.org/10.3767/10.3114/sim.2022.101.05

Swofford DL (2002) PAUP*: phylogenetic analysis using parsimony (*and other methods). Version 4.0b10. Sinauer Associates, Sunderland.

Thompson JD, Gibson TJ, Plewniak F, Jeanmougin F, Higgins DG (1997) The ClustalX windows interface: Fexible strategies for multiple sequence alignment aided by quality analysis tools. Nucleic Acids Research 25(24): 4876–4882. https://doi.org/10.1093/nar/25.24.4876

Tomšovský M (2008) Molecular phylogeny and taxonomic position of *Trametes cervina* and description of a new genus *Trametopsis*. Czech Mycology 60(1): 1–11. https://doi.org/10.33585/cmy.60101

Tomšovský M, Menkis A, Vasaitis R (2010) Phylogenetic relationships in European *Ceriporiopsis* species inferred from nuclear and mitochondrial ribosomal DNA sequences. Fungal Biology 114(4): 350–358. https://doi.org/10.1016/j.funbio.2010.02.004

Westphalen MC, Tomšovský M, Gugliotta AM, Rajchenberg M (2019) An overview of *Antrodiella* and related genera of Polyporales from the Neotropics. Mycologia 111(5): 813–831. https://doi.org/10.1080/00275514.2019.1633895

White TJ, Bruns T, Lee S, Taylor J (1990) Amplification and direct sequencing of fungal ribosomal RNA genes for phylogenetics. In: Innis MA, Gefand DH, Sninsky JJ, White JT (Eds) PCR Protocols: a guide to methods and applications. Academic Press, San Diego, 315–322. https://doi.org/10.1016/B978-0-12-372180-8.50042-1

Wu SH, Nilsson HR, Chen CT, Yu SY, Hallenberg N (2010) The white-rotting genus *Phanerochaete* is polyphyletic and distributed throughout the phleboid clade of the Polyporales (Basidiomycota). Fungal Diversity 42(1): 107–118. https://doi.org/10.1007/s13225-010-0031-7

Wu F, Chen JJ, Ji XH, Vlasák J, Dai YC (2017) Phylogeny and diversity of the morphologically similar polypore genera *Rigidoporus*, *Physisporinus*, *Oxyporus*, and *Leucophellinus*. Mycologia 109: 749–765. https://doi.org/10.1080/00275514.2017.1405215